



## Modeling and Analysis of the Capillary Force for Interactions of Different Tip/Substrate in AFM Based on the Energy Method

Payam, A. F. (2023). Modeling and Analysis of the Capillary Force for Interactions of Different Tip/Substrate in AFM Based on the Energy Method. *ACS Measurement Science Au*, 1-6.  
<https://doi.org/10.1021/acsmesuresciau.3c00001>

[Link to publication record in Ulster University Research Portal](#)

### Published in:

ACS Measurement Science Au

### Publication Status:

Published online: 07/03/2023

### DOI:

[10.1021/acsmesuresciau.3c00001](https://doi.org/10.1021/acsmesuresciau.3c00001)

### Document Version

Publisher's PDF, also known as Version of record

### General rights

Copyright for the publications made accessible via Ulster University's Research Portal is retained by the author(s) and / or other copyright owners and it is a condition of accessing these publications that users recognise and abide by the legal requirements associated with these rights.

### Take down policy

The Research Portal is Ulster University's institutional repository that provides access to Ulster's research outputs. Every effort has been made to ensure that content in the Research Portal does not infringe any person's rights, or applicable UK laws. If you discover content in the Research Portal that you believe breaches copyright or violates any law, please contact [pure-support@ulster.ac.uk](mailto:pure-support@ulster.ac.uk).

# Modeling and Analysis of the Capillary Force for Interactions of Different Tip/Substrate in AFM Based on the Energy Method

Amir Farokh Payam\*

Cite This: <https://doi.org/10.1021/acsmeasuresciau.3c00001>

Read Online

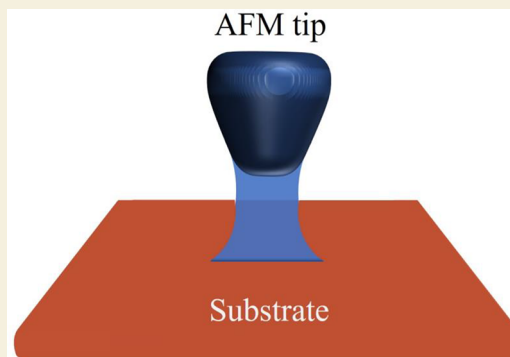
ACCESS |

Metrics &amp; More

Article Recommendations

**ABSTRACT:** This paper presents a simple and robust model to describe the wet adhesion of the AFM tip and substrate joined by a liquid bridge. The effects of contact angles, wetting circle radius, the volume of a liquid bridge, the gap between the AFM tip and substrate, environmental humidity, and tip geometry on the capillary force are studied. To model capillary forces, while a circular approximation for the meniscus of the bridge is assumed, the combination of the capillary adhesion due to the pressure difference across the free surface and the vertical component of the surface tension forces acting tangentially to the interface along the contact line is utilized. Finally, the validity of the proposed theoretical model is verified using numerical analysis and available experimental measurements. The results of this study can provide a basis to model the hydrophobic and hydrophilic tip/surfaces and study their effect on adhesion force between the AFM tip and the substrate.

**KEYWORDS:** Capillary Force, Tip Shape, Humidity, Contact Angles, Meniscus Bridge



## 1. INTRODUCTION

The study of capillary force has a long-time history and is considered a multidisciplinary field of research. Particle coalescence/agglomeration resulting from liquid bridge adhesion plays a significant role in various vital areas such as the pharmaceutical and food industry,<sup>1–3</sup> soft matter and cell biology,<sup>4,5</sup> controlling the fluid flow,<sup>6</sup> and solid–liquid interfaces.<sup>7</sup>

Capillary force is a meniscus force due to condensation typically observed in a wet medium. To model and simulate the capillary force, the nonlinearity of the capillary equation combined with the variety of substrate geometries leads to a large number of solutions.<sup>8–15</sup> Generally, the modeling approaches for capillary force can be classified into two main categories. The first one is based on the integration of the liquid bridge profile with the Laplace–Young equation,<sup>9</sup> while the second approach relies on the total energy of the liquid bridge.<sup>16,17</sup> Due to the simplicity of calculation, the energy approach gets more attention. The usual way to model the capillary force in this approach is a simplification of hydrostatic pressure across the liquid–air interface and subsequently exploits a gorge,<sup>18</sup> circular,<sup>3</sup> parabolic,<sup>19</sup> and toroidal<sup>20</sup> approximation. However, the main limitations of these methods are assumptions or approximations of the bridge profile including distance, volume, and embracing angle.

To measure capillary force, an atomic force microscope (AFM) offers significant advantages and received considerable attention,<sup>3, 10, 11, 16, 21–27</sup> Using different tip shapes, flexible

measurements of materials with various properties, and the possibility of particles glued to the tip apex are the main factors that make AFM a versatile tool for capillary force measurements.<sup>26</sup> To analyze the AFM experimental observables and quantify the measured capillary force, modeling the wet adhesion between different object shapes and particles is required. The basis of most presented models is the energy method or a direct force calculation from the meniscus geometry obtained by the solution of the so-called Laplace equation,<sup>28</sup> consisting of several approximations. For example, Farshchi Tabrizi et al.<sup>24</sup> and Jang et al.<sup>25</sup> assumed equal contact angles for tip/liquid and liquid/plane interfaces in conjunction with a simple geometry for the AFM tip. In another approach, the capillary equation is solved by a numerical algorithm without providing any analytical and mathematical explanation.<sup>23,26</sup>

In this paper, to model the capillary force, I consider either equal or nonequal contact angles for two solid/liquid interfaces, i.e., AFM tip/liquid and liquid/substrate interfaces. Then based on the integration of the capillary adhesion resulting from pressure difference across the free surface and the surface tension force, the different AFM tips in the wet interaction by

**Received:** January 8, 2023

**Revised:** February 22, 2023

**Accepted:** February 23, 2023

the substrate are modeled and analyzed. Hence, in section 2, the formation of the liquid bridge and the energy method is discussed. Then in sections 3 and 4, the capillary force for the two main AFM tip shapes, sphere and two-sphere shape, is calculated.

In section 5, I investigate the effects of the tip/sample distance, humidity, contact angles, and tip geometry on the capillary force for both symmetric and asymmetric cases, and the results of the numerical study are presented. A comparison between the proposed analytical method with the experimental measurement is given in section 6. Finally, in section 7, a conclusion is provided.

## 2. Capillary Force Formation

Figure 1 presents the geometrical schematic of the capillary force problem. Due to the humidity condensation, a tip and plane are

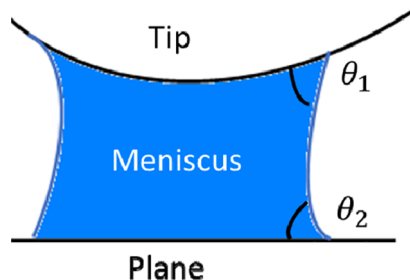


Figure 1. Schematic of the capillary force formation.

linked through a liquid (usually water) meniscus.  $\theta_1$  and  $\theta_2$  are the contact angles for the two-phase interfaces (tip/liquid and liquid/plane).

When the radius of curvature of the nanocontact is below a certain critical radius a meniscus will be formed. This critical radius is defined approximately by the size of the Kelvin radius:

$$\frac{1}{r_{\text{eff}}} = \frac{1}{r_1} + \frac{1}{r_2} \quad (1)$$

Where  $r_1$  and  $r_2$  are the principal radii of the curvature while the former is negative and the latter is positive.<sup>17</sup> The Kelvin radius is connected with the partial pressure  $P_s$  (saturation vapor pressure) by<sup>28</sup>

$$r_{\text{eff}} = \frac{\gamma_l V_m}{R_G T \log\left(\frac{p}{p_s}\right)} \quad (2)$$

With the assumption of the liquid is formed by water vapor,  $\gamma_l = 0.072$  (N/m) is the surface tension,  $R_G = 8.268$  (J/Kmol) is the gas constant,  $T = 298$  (K) is the temperature,  $V_m = 18 \times 10^{-6}$  (m<sup>3</sup>/mol) is the mol volume and  $P/P_s$  is the relative vapor pressure (relative humidity). In general, the meniscus force is the sum of a capillary pressure force caused by the reduced pressure inside the meniscus and the surface tension component, which is a direct result of the surface tension of the liquid.

To describe the shape of the liquid meniscus, the circular approximation,<sup>12,25,29</sup> is assumed. To consider the effect of adhesion force due to the pressure difference between outside and inside the liquid bridge, the energy method is utilized. Subsequently, the capillary force is modeled by the integration of the energy method<sup>30</sup> and the vertical surface tension force.

The capillary pressure energy of a liquid bridge is the sum of two contributions: the liquid–solid ( $\gamma_{sl}A_{sl}$ ), and the solid–vapor

( $\gamma_{sv}A_{sv}$ ) interfacial energies, where  $\gamma$  and  $A$  denote the respective surface tensions and surface areas.

The capillary pressure energy  $W_p$  is given by

$$W_p = - \sum_{1,2} (\gamma_{sl} - \gamma_{sv}) A_{sl} \quad (3)$$

Note that following the methods proposed by previous investigations,<sup>12,24,27</sup> the attractive force is considered to be positive.

Using the Young–Dupré equation, interfacial energies can be substituted by contact angle and surface tension:

$$\gamma_{sv} - \gamma_{sl} = \gamma_{lv} \cos \theta_i \quad i = 1, 2 \quad (4)$$

So the energy equation is converted to

$$W_p = \gamma_{lv} (A_{sl1} \cos \theta_1 + A_{sl2} \cos \theta_2) = \gamma_{lv} A \quad (5)$$

And the capillary force is given by

$$F_c = - \frac{\partial W_p}{\partial D} + F_{st} \quad (6)$$

Where  $F_{st}$  is the surface tension force.

## 3. CAPILLARY FORCE BETWEEN A SPHERE TIP AND A SOLID PLANE

The schematic geometry of a sphere tip and substrate is illustrated in Figure 2.

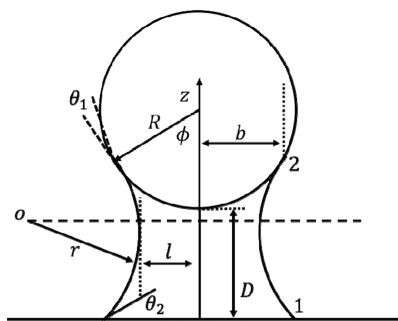


Figure 2. Model for a sphere tip in wet adhesion with a substrate.

In this figure,  $\varphi$  is the filling angle, and  $R$  is the radius of the circle of the liquid bridge wetting the sphere.

The volume of the liquid bridge  $V_l$  is obtained from

$$V_l = \pi R^2 \sin^2 \varphi (D + R(1 - \cos \varphi)) - \frac{\pi}{3} R^3 (1 - \cos \varphi)(2 + \cos \varphi) \quad (7)$$

On the other hand, the relevant areas of eq 5 are given by

$$A_{sl1} = R^2 ((1 - \cos \varphi)^2 + \sin^2 \varphi) \quad (8)$$

$$A_{sl2} = \pi R^2 \sin^2 \varphi \quad (9)$$

$$A = A_{sl1} \cos \theta_1 + A_{sl2} \cos \theta_2 \quad (10)$$

To calculate the capillary force, we need to take the derivative from the energy with respect to the AFM tip and substrate distance. So:

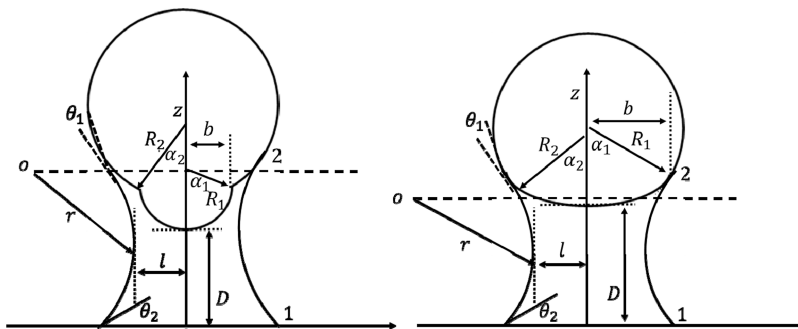


Figure 3. Schematic of a capillary interaction between a two-sphere tip and the plane.

$$F = -2\gamma_{lv}\pi R^2 \sin^2 \varphi (\cos \theta_1 + \cos \varphi \cos \theta_2) \frac{\partial \varphi}{\partial D} + 2\pi\gamma_{lv}R \sin \varphi \sin(\varphi + \theta_1) \quad (11)$$

Note that  $\partial\varphi/\partial D$  is calculated based on the following condition:

$$\frac{\partial V_1}{\partial D} = 0 \quad (12)$$

So,  $\partial\varphi/\partial D$  is obtained as

$$\frac{\partial \varphi}{\partial D} = \frac{\tan \varphi}{2R(1 - \cos \varphi) \left(1 + \frac{D}{d}\right)} \quad (13)$$

Where

$$d = R(1 - \cos \varphi) \quad (14)$$

Substituting  $\partial\varphi/\partial D$  in (11), the capillary force is calculated by

$$F = \frac{-\gamma_{lv}\pi R(1 + \cos \varphi)(\cos \theta_1 + \cos \varphi \cos \theta_2)}{\cos \varphi(1 + D/d)} + 2\pi\gamma_{lv}R \sin \varphi \sin(\varphi + \theta_1) \quad (15)$$

It is worth mentioning that the presented model is limited by the value of the filling angle to be in the range that the calculated relative humidity does not increase by more than 1, which has no physical meaning.

#### 4. CAPILLARY FORCE BETWEEN A TWO-SPHERE TIP AND A SOLID PLANE

The schematic of the analysis model for a sphere tip and the flat substrate is shown in Figure 3. In this figure, the radius of spheres is depicted by  $R_1$ ,  $R_2$ ;  $\alpha_1$  is the maximum of the half opening angle of the part of sphere 1, and  $\alpha_2$  is the minimum half of the opening angle of sphere 2;  $b$  is the circle radius of the water meniscus wetting the sphere tip; and  $D$  is the distance between tip and substrate.

For  $b < R_1 \sin \alpha_1 = R_2 \sin \alpha_2$ , the liquid bridge is formed between the first spherical end of the tip and substrate ( $R_1$ ). For this case, the procedure is identical to the case of sphere tip in section 3.

For  $b \geq R_1 \sin \alpha_1 = R_2 \sin \alpha_2$  the liquid bridge is formed on the sphere 2 boundary. In this case, the volume becomes

$$V_l = \pi(R_2(\cos \alpha_2 - \cos \phi_2) + D + R_1(1 - \cos \alpha_1))(R_2^2 \sin^2 \phi_2) - \frac{\pi}{6} \left( R_2^3(1 - \cos \phi_2)(3(\sin \phi_2)^2 + (1 - \cos \phi_2)^2) - R_1^3(1 - \cos \alpha_2)(3(\sin \alpha_2)^2 + (1 - \cos \alpha_2)^2) + R_1^3(1 - \cos \alpha_1)(3(R_2^2 \sin \alpha_2)^2 + R_1^2(1 - \cos \alpha_1)^2) \right) \quad (16)$$

The relevant areas for the eq 5 are given by

$$A_{sl1} = \pi(R_2^2(\sin^2 \varphi_2 + (1 - \cos \varphi_2)^2) - R_2^2((1 - \cos \alpha_2)^2 + \sin^2 \alpha_2) + (R_1^2(1 - \cos \alpha_1)^2 + R_2^2 \sin^2 \alpha_2)) \quad (17)$$

$$A_{sl2} = \pi R_2^2 \sin^2 \varphi_2 \quad (18)$$

To calculate the capillary force, we need to take the derivative of the energy with respect to the distance:

$$F_c = -\frac{\partial W_{cp}}{\partial D} + F_{st} = -\gamma_{lv} \left( \frac{\partial A}{\partial \varphi_2} \frac{\partial \varphi_2}{\partial D} + \frac{\partial A}{\partial D} \right) + 2\pi\gamma_{lv}R_2 \sin \varphi_2 \sin(\varphi_2 + \theta_2) \quad (19)$$

$\partial\varphi_2/\partial D$  is calculated based on the following condition:

$$\frac{\partial V_l}{\partial D} = \frac{\partial V_l}{\partial \varphi_2} \frac{\partial \varphi_2}{\partial D} + \frac{\partial V_l}{\partial D} = 0 \quad (20)$$

Substituting  $\partial\varphi_2/\partial D$  in (19), the capillary force is calculated.

## 5. NUMERICAL RESULTS AND DISCUSSION

### 5.1. Spherical Tip and Substrate

Figure 4 illustrates the relationship between the AFM tip, the distance between the tip and substrate, and capillary force. By

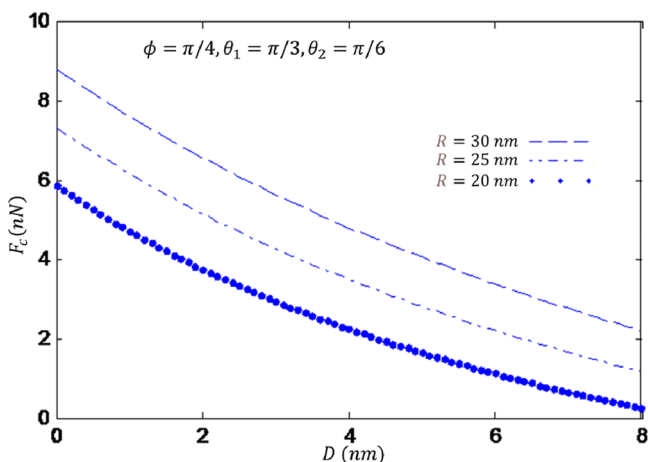


Figure 4. Capillary force as a function of the distance between tip and substrate.

increasing the distance, the capillary force is reduced. Also, decreasing the sphere tip radius leads to a reduction in capillary force.

Figure 5 shows the dependency of capillary force on the humidity. In this case, I consider the effects of contact angles. So,

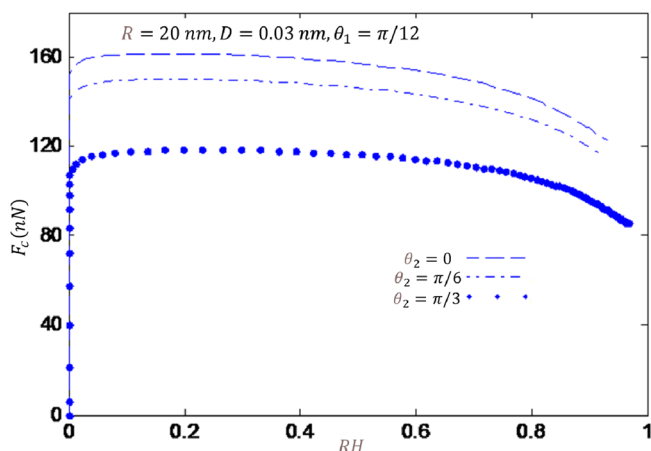


Figure 5. Capillary force versus humidity for different contact angles.

by keeping the fixed distance between the tip and substrate, the contact angles are changed. From the results, I conclude that as the contact angle between the substrate and liquid increases, the capillary force decreases. So, hydrophobicity of the surface leads to a reduction of capillary forces.

Furthermore, for all three different contact angles, the trend of capillary force behavior with changes in relative humidity is the same. As the results show, increasing the relative humidity first increases the capillary force, then at higher relative humidity, the capillary force decreases.

### 5.2. Two-Sphere Tip and Substrate

In this numerical analysis, I consider two cases. In the first case, I select a sharp tip. As Figure 6 shows, by increasing the humidity, the capillary force increases. Also, the results demonstrate the transition region between the two radii. The results of the second case are reported in Figure 7 as I consider the blunt tip. Here, I use the two-sphere model to calculate the capillary force.

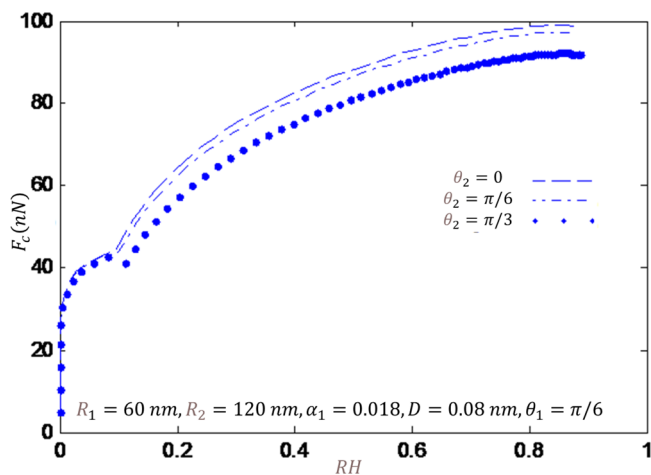


Figure 6. Capillary force versus humidity for a sharp tip and different contact angles.

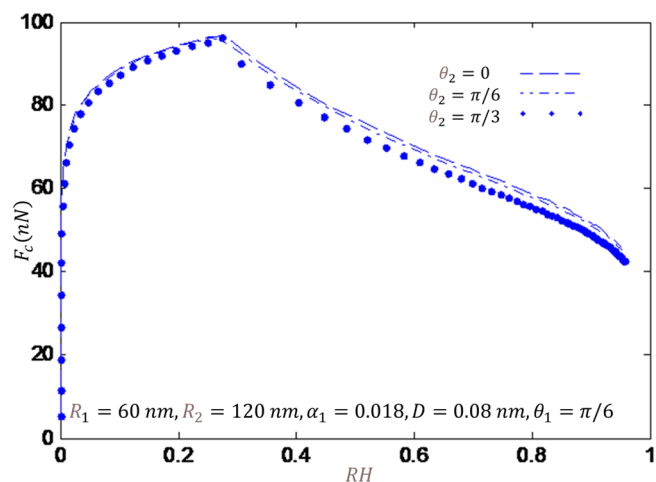


Figure 7. Capillary force versus humidity for a blunt tip and several contact angles.

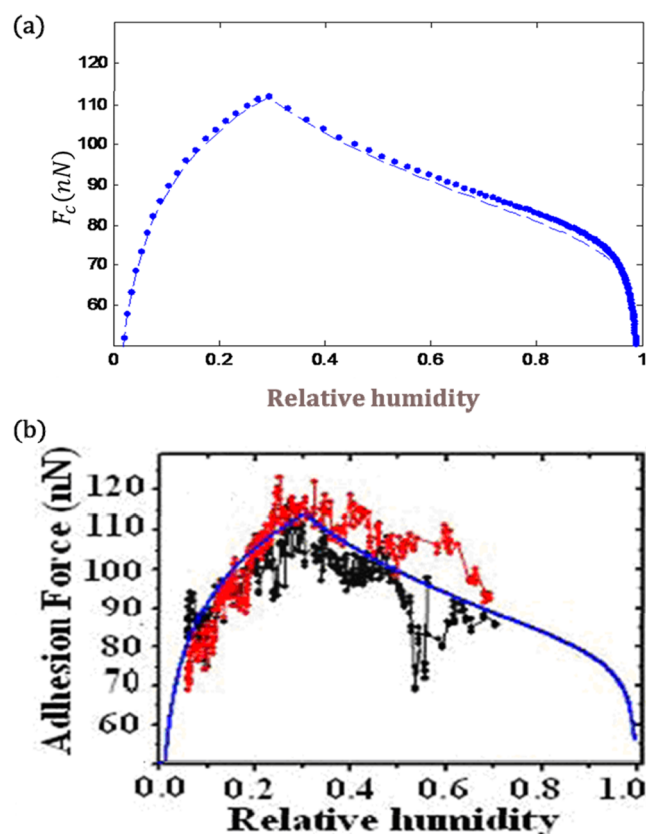


Figure 8. (a) The simulation of the experimental measurement in refs 24,31 with the presented model and comparison with the (b) experimental measurements. Reprinted (adapted) with permission from ref 24 [Langmuir 2006, 22, (S), 2171–2184]. Copyright {2006} American Chemical Society.

From these results, one may infer when the wet circle boundary is located on the first sphere, the capillary force increases as the humidity increases. In contrast, in the transition region between two spheres, the capillary force decreases by increasing the humidity. From these results, it can be inferred that in the case of the two-sphere model, the effect of relative humidity on capillary force is dependent on the tip shape. For the sharp tip, increasing relative humidity leads to an increase of capillary force. While for the blunt tip, the same as the sphere tip,

the capillary force decreases by increasing the relative humidity. Furthermore, according to the physical understanding, a decrease in the contact angles and the gap between the tip and substrate increases the capillary force. This result can explain the observed behavior of the hydrophilic surface in increasing the capillary force.

## 6. COMPARISON WITH EXPERIMENTAL RESULTS

In this section, to examine the validity of the presented approach, I regenerate the experimental curves of adhesion force versus humidity. As can be seen, high proximity exists between the proposed model and the experimental measurements. It is worthwhile to mention that Figure 8 (—) is taken from<sup>31</sup> and regenerated here for comparison purposes. The simulation parameters are selected from the experimental measurements of ref.<sup>31</sup> As shown in Figure 3.11-C of ref.<sup>31</sup> the tip shape can be modeled as a two-sphere shape (Figure 3).

## 7. CONCLUSION

In this paper by considering two main AFM tip shapes and a flat substrate, based on the combination of energy method to calculate adhesion forces due to the Laplace pressure and surface tension force, the capillary adhesion force is calculated. The basis of the models is a circular interface in a radial cross-section. In addition to simplicity and robustness, the main advantage of the proposed method is the analytical solution of capillary force equations while avoiding several approximations considered in the previous analytical approaches. Moreover, as an advantage of the proposed approach, we can model the symmetric and asymmetric cases for the meniscus geometry as representative of hydrophilic and hydrophobic surfaces. Finally, by the numerical analysis and comparison with the available measurement data, derived models are examined, and I verify the accuracy and precision of the calculations.

## AUTHOR INFORMATION

### Corresponding Author

Amir Farokh Payam – Nanotechnology and Integrated Bioengineering Centre (NIBEC), School of Engineering, Ulster University, Belfast BT15 1AP, United Kingdom;  
Email: a.farokh-payam@ulster.ac.uk

Complete contact information is available at:  
<https://pubs.acs.org/10.1021/acsmeasuresciau.3c00001>

### Notes

The author declares no competing financial interest.

## ACKNOWLEDGMENTS

This work is supported by Department for Economy, Northern Ireland through US-Ireland R&D partnership grant No. USI 186.

## REFERENCES

- (1) Li, S.; Marshall, J. S.; Liu, G.; Yao, Q. Adhesive particulate flow: The discrete-element method and its application in energy and environmental engineering. *Prog. Energy Combust. Sci.* **2011**, *37* (6), 633–668.
- (2) Toschkoff, G.; Khinast, J. G. Mathematical modeling of the coating process. *Int. J. Pharm.* **2013**, *457* (2), 407–422.
- (3) Chen, S. H.; Soh, A. K. The capillary force in micro- and nano-indentation with different indenter shapes. *Int. J. Solids Struct.* **2008**, *45* (10), 3122–3137.
- (4) Dudukovic, N. A.; et al. Cellular fluidics. *Nature* **2021**, 595 (7865), 58–65.
- (5) Gouveia, B.; Kim, Y.; Shaevitz, J. W.; Petry, S.; Stone, H. A.; Brangwynne, C. P. Capillary forces generated by biomolecular condensates. *Nature* **2022**, *609* (7926), 255–264.
- (6) van Neel, T. L.; Theberge, A. B. Programmable capillary action controls fluid flows. *Nature* **2021**, *595* (7865), 31–32.
- (7) Payam, A. F.; Kim, B.; Lee, D.; Bhalla, N. Unraveling the liquid gliding on vibrating solid liquid interfaces with dynamic nanoslip enactment. *Nat. Commun.* **2022**, *13* (1), 6608.
- (8) Nguyen, H. N. G.; Zhao, C. F.; Millet, O.; Selvadurai, A. P. S. Effects of surface roughness on liquid bridge capillarity and droplet wetting. *Powder Technol.* **2021**, *378*, 487–496.
- (9) Kruyt, N. P.; Millet, O. An analytical theory for the capillary bridge force between spheres. *J. Fluid Mech.* **2017**, *812*, 129–151.
- (10) Farrokh Payam, A.; Fathipour, M. Capillary force models for interactions of several Tip/Substrate in AFM based on the energy method. *J. Surf. Sci. Technol.* **2012**, *28* (1–2), 71–90.
- (11) Stifter, T.; Marti, O.; Bhushan, B. Theoretical investigation of the distance dependence of capillary and van der Waals forces in scanning force microscopy. *Phys. Rev. B - Condens. Matter Mater. Phys.* **2000**, *62* (20), 13667–13673.
- (12) Yoon, E. S.; Yang, S. H.; Han, H. G.; Kong, H. An experimental study on the adhesion at a nano-contact. *Wear* **2003**, *254* (10), 974–980.
- (13) Sun, X.; Sakai, M. A liquid bridge model for spherical particles applicable to asymmetric configurations. *Chem. Eng. Sci.* **2018**, *182*, 28–43.
- (14) Wu, D.; Zhou, P.; Wang, G.; Zhao, B.; Howes, T.; Chen, W. Modeling of capillary force between particles with unequal contact angle. *Powder Technol.* **2020**, *376*, 390–397.
- (15) Goodband, S. J.; Kusumaatmaja, H.; Voitchovsky, K. Development of a setup to characterize capillary liquid bridges between liquid infused surfaces. *AIP Adv.* **2022**, *12* (1), 015120.
- (16) Rabinovich, Y. I.; Esayanur, M. S.; Moudgil, B. M. Capillary forces between two spheres with a fixed volume liquid bridge: Theory and experiment. *Langmuir* **2005**, *21* (24), 10992–10997.
- (17) Payam, A. F.; Fathipour, M. A capillary force model for interactions between two spheres. *Particuology* **2011**, *9* (4), 381–386.
- (18) Gras, J. P.; Delenne, J. Y.; El Youssoufi, M. S. Study of capillary interaction between two grains: A new experimental device with suction control. *Granul. Matter* **2013**, *15* (1), 49–56.
- (19) Shi, D.; McCarthy, J. J. Numerical simulation of liquid transfer between particles. *Powder Technol.* **2008**, *184* (1), 64–75.
- (20) Zhao, C. F.; Kruyt, N. P.; Millet, O. Capillary bridges between spherical particles under suction control: Rupture distances and capillary forces. *Powder Technol.* **2020**, *360*, 622–634.
- (21) Payam, A. F.; Jalalifar, M.; Fathipour, M. Modeling and Analysis of Capillary Force Interaction for Common AFM Tip Shapes. *World Appl. Sci. J.* **2012**, *16* (12), 1803–1814.
- (22) Sirghi, L.; Nakagiri, N.; Sugisaki, K.; Sugimura, H.; Takai, O. Effect of sample topography on adhesive force in atomic force spectroscopy measurements in air. *Langmuir* **2000**, *16* (20), 7796–7800.
- (23) Chau, A.; Rignier, S.; Delchambre, A.; Lambert, P. Three-dimensional model for capillary nanobridges and capillary forces. *Model. Simul. Mater. Sci. Eng.* **2007**, *15* (3), 305–317.
- (24) Farshchi-Tabrizi, M.; Kappl, M.; Cheng, Y.; Gutmann, J.; Butt, H. J. On the adhesion between fine particles and nanocontacts: An atomic force microscope study. *Langmuir* **2006**, *22* (5), 2171–2184.
- (25) Jang, J.; Schatz, G. C.; Ratner, M. A. Capillary force in atomic force microscopy. *J. Chem. Phys.* **2004**, *120* (3), 1157–1160.
- (26) Pakarinen, O. H.; et al. Towards an accurate description of the capillary force in nanoparticle-surface interactions. *Model. Simul. Mater. Sci. Eng.* **2005**, *13* (7), 1175–1186.
- (27) Chen, Y.; Zhao, Y.; Gao, H.; Zheng, J. Liquid bridge force between two unequal-sized spheres or a sphere and a plane. *Particuology* **2011**, *9* (4), 374–380.

(28) Israelachvili, J. N. *Intermolecular and Surface Forces*; Academic Press: London, 1992.

(29) Marmur, A. Tip-Surface Capillary Interactions. *Langmuir* **1993**, *9* (7), 1922–1926.

(30) De Souza, E. J. The effect of capillary forces on adhesion of biological and artificial attachment devices. Ph.D. Thesis, Max-Planck-Institut für Metallforschung, September, 2007.

(31) Farshchi-Tabrizi, M. *On the Adhesion between Fine Particles and Nanocontacts: An Atomic Force Microscope Study*. Universität Siegen, January, 2007.

## Recommended by ACS

### Surface Passivation of Niobium Superconducting Quantum Circuits Using Self-Assembled Monolayers

Mohammed Alghadeer, Saleem Ghaffar Rao, *et al.*

DECEMBER 27, 2022  
ACS APPLIED MATERIALS & INTERFACES

READ 

### Long-Range Electrification of an Air/Electrolyte Interface and Probing Potential of Zero Charge by Conductive Amplitude-Modulated Atomic Force Microscopy

Thanh Duc Dinh, Seongpil Hwang, *et al.*

JANUARY 23, 2023  
ANALYTICAL CHEMISTRY

READ 

### Influence of Matrix $pK_a$ on Molecular Ion Formation in Matrix-Enhanced Secondary-Ion Mass Spectrometry

Yogesh Pohkrel, Bonnie J. Tyler, *et al.*

DECEMBER 24, 2022  
JOURNAL OF THE AMERICAN SOCIETY FOR MASS SPECTROMETRY

READ 

### Optimizing the Ferroelectric Properties of $Hf_{1-x}Zr_xO_2$ Films via Crystal Orientation

Chih-Yu Teng, Yuan-Chieh Tseng, *et al.*

FEBRUARY 07, 2023  
ACS APPLIED ELECTRONIC MATERIALS

READ 

Get More Suggestions >